

Power-Bus Sensitivity Analysis

Luca De Camillis, Giulio Antonini, *Senior Member, IEEE*, and Vikram Jandhyala, *Senior Member, IEEE*

Abstract—Design of modern printed circuit boards requires robust simulation techniques to model power-bus structures. A reliable method is the cavity model which assumes small spacing between power and ground planes. Designers often make the proper tradeoffs between conflicting design requirements using optimization techniques, to obtain the best possible performance. To this aim, sensitivity information with respect to power-bus parameters are required by optimizers which employ gradient-based techniques and need the knowledge of sensitivities of the output responses. In this paper, the sensitivity analysis of power-bus structures is presented. Relying on the cavity model, voltage sensitivity is computed in a rational function form or rational polynomial form leading to a time-domain macromodel which can be efficiently interfaced with linear and nonlinear terminations or Spice-like simulators. The simulation results show the accuracy of the proposed approach.

Index Terms—Power-bus, sensitivity analysis, transient analysis.

I. INTRODUCTION

MULTILAYER printed circuit boards (PCBs) usually employ entire layers for power and ground planes delivering dc power distribution for integrated circuits (ICs) operating at high speeds. The power-ground planes may represent an important noise coupling path leading to signal integrity (SI) and electromagnetic interference/compatibility (EMI/C) problems [1], [2]. As a result, power-bus noise has become a major concern for EMI/C engineers in PCB designs.

Power-bus structures can be efficiently modeled by full-wave techniques such as the finite-difference time-domain (FDTD) method [3] or the partial element equivalent circuit (PEEC) [4] approach which are usually time and memory consuming. A valuable alternative is represented by the cavity-mode model which has also been used to characterize the rectangular power-bus structure as a multiport microwave circuit [5], [6]. This model permits analytical computation of the impedance matrix Z of rectangular power-bus structures as a double infinite series. The rational form or rational polynomial form of each term of the summation allows to easily generate a state-space macromodel which is well suited for time-domain

Manuscript received January 29, 2009; revised March 20, 2009. This work was supported by the Italian Ministry of University (MIUR) under a Program for the Development of Research of National Interest (PRIN Grant 2006095890). This work was recommended for publication by Associate Editor M. Cases upon evaluation of the reviewers comments.

G. Antonini and L. De Camillis are with the UAq EMC Laboratory, Dipartimento di Ingegneria Elettrica e dell'Informazione, Università degli Studi dell'Aquila, 67040 L'Aquila, Italy (e-mail: antonini@ing.univaq.it).

V. Jandhyala is with the Department of Electrical Engineering, Paul Allen Center, University of Washington, Seattle, WA 98185 USA (e-mail: vj@u.washington.edu).

Color versions of one or more of the figures in this paper are available online at <http://ieeexplore.ieee.org>.

Digital Object Identifier 10.1109/TADVP.2009.2022322

simulations [7]. For irregular shapes, the segmentation method can be employed [8]–[11]. A vast literature is available on the improvements of the method, dealing with the convergence speedup of the series [12]–[15], modeling of fringing fields [16]–[18], incorporation of radiation losses [19], [20].

Due to the inadequacies in state-of-the-art electronic design automation tools, physical layout of most analog functions is still done manually. Designers usually rely on experience in making layouts and detecting layout problems. Despite this experience, they very often need to go through many iterations to bring the physical design within the specifications. This does not coincide with the digital VLSI design automation trends. This results in a dramatic reduction in productivity and an increase in the design cycle time.

A tool that is able to pinpoint the important layout-related parameters and quantify their effect on the performance functions can be of great help. Being aware of the relative importance of the parameters, a designer can then modify the layout in a way to reduce the effect of critical parameters. This has the effect of reducing the physical design iterations. Also, this can be of great help in building a more effective layout methodology for analog circuits.

This paper discusses the importance of using sensitivity analysis as a response to the aforementioned need. Sensitivities quantify the performance degradation induced by changes in different design and process parameters. Hence, critical parameters can be easily detected. In this way, the layout design can be controlled in order to avoid excessive changes in these parameters.

The paper is organized as follows. In Section II the computation of the voltage sensitivity in terms of the closed-form Green's function for voltages via planar-circuit approach is presented. Section III discusses the different parameter (port positions and geometrical parameters) used in this work and the computation of the corresponding sensitivities is presented in Section IV. The time-domain macromodel is developed in Section V. Several examples, in both the time and frequency-domain, are presented in Section VI, confirming the capability of the proposed approach to provide a fast and reliable method to sensitivity of power-bus structures.

II. ELECTRICAL MODEL FOR MODAL PROPAGATION

In the setup of CAD techniques, the compromise between accuracy and simplicity is a stringent requirement. Exact analyses are often impractical because of the exceedingly high computer time required. From this perspective, the planar-circuit approach is a very powerful technique, which has been basically developed for the analysis of microstrip circuits, but can be extended to other microwave circuit configurations, such as reduced-height waveguide, striplines, suspended microstrips, etc.

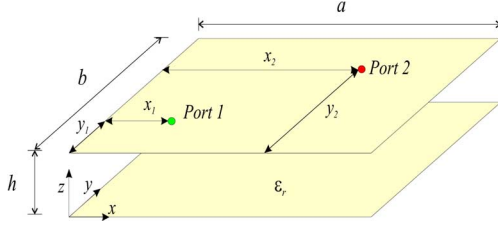


Fig. 1. Schematic of a two-layer power-bus structure.

A planar circuit is defined as an electrical circuit having two dimensions comparable with the wavelength, while the third dimension is a negligible fraction of the wavelength. Though the planar circuit is an approximate model of microstrip components, it constitutes a substantial improvement over conventional transmission-line models, providing accurate descriptions of their performances. On the other hand, planar-circuit models are simple enough to keep computer analysis reasonably inexpensive. A sample of a power-bus structure is sketched in Fig. 1.

As will be shown, a 2-D circuit theory can be developed for planar components by extending to the 2-D case the concepts of voltage and current usually defined in transmission-line theory.

Because of planarity ($\partial/\partial z = 0$) and open-circuit boundary conditions, Maxwell's equations, in the Laplace domain, reduce to [9]

$$\nabla_t E_z(\mathbf{r}) = -s\mu\hat{z} \times \mathbf{H}_t(\mathbf{r}) \quad (1)$$

$$\nabla_t \times \mathbf{H}_t(\mathbf{r}) = (s\epsilon E_z(\mathbf{r}) + J_z(\mathbf{r})) \quad (2)$$

where ∇_t is the 2-D nabla operator, \hat{z} is the unit vector normal to the plane of the circuit, μ and ϵ are the permeability and permittivity of the filling substrate material. The E -field has only the z -component, while the H -field lies in the xy plane.

A 2-D form of telegraphers' equations can be obtained from (1) and (2) defining at each point \mathbf{r} of the planar circuit a voltage $v(\mathbf{r})$ and a surface current density $\mathbf{J}_s(\mathbf{r})$ flowing on the top conductor as

$$v(\mathbf{r}) = -hE_z(\mathbf{r}) \quad (3)$$

$$\mathbf{J}_s(\mathbf{r}) = -\hat{z} \times \mathbf{H}_t(\mathbf{r}). \quad (4)$$

Inserting (3) and (4) into (1) and (2), we get

$$\nabla_t v(\mathbf{r}) = -Z_e \mathbf{J}_s(\mathbf{r}) \quad (5)$$

$$\nabla_t \cdot \mathbf{J}_s(\mathbf{r}) = -Y_s v(\mathbf{r}) + J_z(\mathbf{r}) \quad (6)$$

in which we have considered

$$Z_e = s\mu h \quad (7)$$

$$Y_s = s\frac{\epsilon}{h}. \quad (8)$$

We can define the input current vector by multiplying the density current vector to ab . In this way, multiplying and dividing the $J_z(\mathbf{r})$ term into (6) by ab we obtain

$$\nabla_t \cdot \mathbf{J}_s(\mathbf{r}) = -Y_s v(\mathbf{r}) + J_z(\mathbf{r}). \quad (9)$$

Differentiating (5) and (9) with respect to a parameter λ (where λ represents any electrical or physical interconnect parameter of interest) yields the following relationship:

$$\frac{d}{d\lambda} (\nabla_t v(\mathbf{r})) = \frac{d}{d\lambda} (-Z_e \mathbf{J}_s(\mathbf{r})) \quad (10)$$

$$\frac{d}{d\lambda} (\nabla_t \cdot \mathbf{J}_s(\mathbf{r})) = \frac{d}{d\lambda} (-Y_s v(\mathbf{r})) + \frac{d}{d\lambda} J_z(\mathbf{r}). \quad (11)$$

Now, using Schwarz's theorem, we can commute the derivative with the nabla operator such that

$$\nabla_t \hat{v}(\mathbf{r}) = -\frac{dZ_e}{d\lambda} \mathbf{J}_s(\mathbf{r}) - Z_e \hat{\mathbf{J}}_s(\mathbf{r}) \quad (12)$$

$$\nabla_t \cdot \hat{\mathbf{J}}_s(\mathbf{r}) = -\frac{dY_s}{d\lambda} v(\mathbf{r}) - Y_s \hat{v}(\mathbf{r}) + \frac{d}{d\lambda} J_z(\mathbf{r}) \quad (13)$$

in which we have defined the sensitivity variables as

$$\hat{v}(\mathbf{r}) = \frac{d}{d\lambda} v(\mathbf{r}) \quad (14)$$

$$\hat{\mathbf{J}}_s(\mathbf{r}) = \frac{d}{d\lambda} \mathbf{J}_s(\mathbf{r}). \quad (15)$$

If we apply the divergence at (12) we obtain

$$\nabla_t \cdot \nabla_t \hat{v}(\mathbf{r}) = -\nabla_t \cdot \left[\frac{dZ_e}{d\lambda} \cdot \mathbf{J}_s(\mathbf{r}) \right] - \nabla_t \cdot [Z_e \hat{\mathbf{J}}_s(\mathbf{r})] \quad (16)$$

and so, with the vector identity $\nabla \cdot (\phi \underline{A}) = \nabla \phi \cdot \underline{A} + \phi \nabla \cdot \underline{A}$, the following:

$$\begin{aligned} \nabla_t^2 \hat{v}(\mathbf{r}) = & -\nabla_t \cdot \left(\frac{dZ_e}{d\lambda} \right) \cdot \mathbf{J}_s(\mathbf{r}) - \frac{dZ_e}{d\lambda} \nabla_t \cdot \mathbf{J}_s(\mathbf{r}) \\ & -\nabla_t Z_e \cdot \hat{\mathbf{J}}_s(\mathbf{r}) - Z_e \nabla_t \cdot \hat{\mathbf{J}}_s(\mathbf{r}). \end{aligned} \quad (17)$$

The terms $-\nabla_t (dZ_e/d\lambda) \cdot \mathbf{J}_s(\mathbf{r})$ and $-\nabla_t Z_e \cdot \hat{\mathbf{J}}_s(\mathbf{r})$ are equal to zero, because the impedance Z_e and the admittance Y_s does not depend on x, y . Thus, substituting (9) and (13) into (17), we obtain

$$\nabla_t^2 \hat{v}(\mathbf{r}) - \gamma^2 \hat{v}(\mathbf{r}) = \frac{d\gamma^2}{d\lambda} v(\mathbf{r}) - \frac{dZ_e}{d\lambda} J_z(\mathbf{r}) - Z_e \frac{dJ_z(\mathbf{r})}{d\lambda} \quad (18)$$

where

$$\gamma^2 = Z_e Y_s \quad (19a)$$

$$\frac{d\gamma^2}{d\lambda} = \left(Z_e \frac{dY_s}{d\lambda} + Y_s \frac{\partial Z_e}{\partial \lambda} \right) \quad (19b)$$

$$\begin{aligned} J_z(\mathbf{r}) = & I_{z0} \delta(\mathbf{r} - \mathbf{r}_0) + I_{z1} \delta(\mathbf{r} - \mathbf{r}_1) + \dots \\ & + I_{zl} \delta(\mathbf{r} - \mathbf{r}_l) \end{aligned} \quad (19c)$$

and $\delta(\mathbf{r})$ is a bi-dimensional Dirac delta function.

Equation (18) represents a Sturm-Liouville problem for the sensitivity \hat{v} ; its solution can be computed in terms of the Green's function as

$$\hat{v}(\mathbf{r}) = \int_S G(\mathbf{r}, \mathbf{r}') f(\mathbf{r}') dS \quad (20)$$

where

$$f(\mathbf{r}') = \frac{d\gamma^2}{d\lambda} v(\mathbf{r}') - \frac{dZ_e}{d\lambda} J_z(\mathbf{r}') - Z_e \frac{dJ_z(\mathbf{r}')}{d\lambda}. \quad (21)$$

For a rectangular plane structure with dimension $a \times b$, separated by a dielectric of thickness $h \ll \lambda_{\min}$ (λ_{\min} being the minimum wavelength in the frequency range of interest), the Green's function can be computed as in [21] and shown in (22b)

$$\begin{aligned} G(\mathbf{r}, \mathbf{r}') &= - \sum_{m=0}^{\infty} \sum_{n=0}^{\infty} \Phi_{mn}(s) N_{mn}(\mathbf{r}) N_{mn}(\mathbf{r}') \quad (22a) \\ N_{mn}(\mathbf{r}) &= \sqrt{C_m} \sqrt{C_n} \cos\left(\frac{m\pi x_r}{a}\right) \cdot \cos\left(\frac{n\pi y_r}{b}\right) \\ N_{mn}(\mathbf{r}') &= \sqrt{C_m} \sqrt{C_n} \cos\left(\frac{m\pi x_{r'}}{a}\right) \cdot \cos\left(\frac{n\pi y_{r'}}{b}\right) \\ \Phi_{mn}(s) &= \frac{1}{(k_{mn}^2 - k^2)ab} \quad (22b) \end{aligned}$$

where (x_r, y_r) are the coordinates at the center of the \mathbf{r} -port, (t_{xr}, t_{yr}) are the dimensions of the \mathbf{r} -port, $k = \omega\sqrt{\mu\epsilon}$, $k_{mn}^2 = (m\pi/a)^2 + (n\pi/b)^2$, $C_m = 1$ if $m = 0$, $C_m = 2$ if $m \neq 0$, m represents the m th mode associated with the x -dimension, and n represents the n th mode associated with the y -dimension.

III. SENSITIVITY PARAMETERS

Let us consider the sensitivity parameter λ . In order to compute the sensitivity (20) we need to consider the forcing term (21) and the expressions of the terms therein. The derivative in (21) can assume different expression depending on the particular selected sensitivity parameter. Let us consider two cases:

- 1) λ as the position of one or more ports on the power-bus;
- 2) λ as a geometrical or electrical parameter.

In order to simplify the calculus, we can decompose the forcing term (21) into three terms. Let us consider $f(\mathbf{r}') = F_1(\mathbf{r}') + F_2(\mathbf{r}') + F_3(\mathbf{r}')$, as

$$\begin{aligned} F_1(\mathbf{r}') &= \frac{d\gamma^2}{d\lambda} v(\mathbf{r}') & F_2(\mathbf{r}') &= -\frac{dZ_e}{d\lambda} J_z(\mathbf{r}') \\ F_3(\mathbf{r}') &= -Z_e \frac{dJ_z(\mathbf{r}')}{d\lambda}. \end{aligned} \quad (23)$$

A. Position of Ports

To compute the sensitivity parameter with respect to the position of one or more ports we need to define $2l$ variables if we have l ports $\mathbf{r}_0, \mathbf{r}_1, \dots, \mathbf{r}_l$ that is $(x_0, y_0), (x_1, y_1), \dots, (x_l, y_l)$. This is because variation of these ports is independent from the others, and should be evaluated as the derivative with respect to the correlated variable. For example, the voltage sensitivity at port i with respect to the variation of port j reads

$$\hat{v}(\mathbf{r}_i) = \frac{dv(\mathbf{r}_i)}{d\mathbf{r}_j}. \quad (24)$$

For the sake of simplicity, in the following we consider the variation of one port as a single sensitivity parameter, $\lambda = \mathbf{r}_j$. In this way the sensitivity can be evaluated as in (24).

Now, let us consider the forcing term in (39). As stated before, γ^2 and Z_e do not depend on $\lambda = \mathbf{r}_j$ and, thus, the F_1 and F_2 terms are equal to zero. The F_3 term reads

$$\begin{aligned} F_3(\mathbf{r}') &= -Z_e \frac{dJ_z(\mathbf{r}')}{d\mathbf{r}_j} \\ &= -Z_e \left[\frac{d}{d\mathbf{r}_j} (I_{z0}\delta(\mathbf{r}' - \mathbf{r}_0)) \right. \\ &\quad \left. + \frac{d}{d\mathbf{r}_j} (I_{z1}\delta(\mathbf{r}' - \mathbf{r}_1)) + \dots \right. \\ &\quad \left. + \frac{d}{d\mathbf{r}_j} (I_{zl}\delta(\mathbf{r}' - \mathbf{r}_l)) \right] \\ &= -Z_e \left[\frac{dI_{z0}}{d\mathbf{r}_j} \delta(\mathbf{r}' - \mathbf{r}_0) + \dots + \frac{dI_{zl}}{d\mathbf{r}_j} \delta(\mathbf{r}' - \mathbf{r}_l) \right. \\ &\quad \left. + I_{z0} \frac{d\delta(\mathbf{r}' - \mathbf{r}_0)}{d\mathbf{r}_j} + \dots + I_{zl} \frac{d\delta(\mathbf{r}' - \mathbf{r}_l)}{d\mathbf{r}_j} \right] \\ &= -Z_e (F_3^{(1)} + F_3^{(2)}) \quad (25) \end{aligned}$$

in which we have defined

$$F_3^{(1)}(\mathbf{r}') = \frac{dI_{z0}}{d\mathbf{r}_j} \delta(\mathbf{r}' - \mathbf{r}_0) + \dots + \frac{dI_{zl}}{d\mathbf{r}_j} \delta(\mathbf{r}' - \mathbf{r}_l) \quad (26)$$

$$F_3^{(2)}(\mathbf{r}') = I_{z0} \frac{d\delta(\mathbf{r}' - \mathbf{r}_0)}{d\mathbf{r}_j} + \dots + I_{zl} \frac{d\delta(\mathbf{r}' - \mathbf{r}_l)}{d\mathbf{r}_j}. \quad (27)$$

In order to compute (25) we require two properties of the Dirac delta function [22]

$$\int_{-\infty}^{+\infty} h(z)\delta(z-a)dz = h(a) \quad (28)$$

$$\int_{-\infty}^{+\infty} \delta'(z-a)h(z)dz = -h'(a) \quad (29)$$

where the $'$ symbol stands for the derivative with respect to z and for all continuous $h(z)$.

To compute the response in (26) we need (28). The result reads

$$\begin{aligned} &\int_S G(\mathbf{r}, \mathbf{r}') F_3^{(1)}(\mathbf{r}') dS \\ &= G(\mathbf{r}, \mathbf{r}_0) \frac{dI_{z0}}{d\lambda} + \dots + G(\mathbf{r}, \mathbf{r}_l) \frac{dI_{zl}}{d\lambda} \\ &= \tilde{G}(\mathbf{r}) \frac{d\tilde{I}_z}{d\lambda} \quad (30) \end{aligned}$$

where

$$\tilde{G}(\mathbf{r}) = [G(\mathbf{r}, \mathbf{r}_0) \quad G(\mathbf{r}, \mathbf{r}_1) \quad \dots \quad G(\mathbf{r}, \mathbf{r}_l)] \quad (31a)$$

$$\tilde{I}_z = [I_{z0}, I_{z1}, \dots, I_{zl}]^T \quad (31b)$$

$$\frac{d\tilde{I}_z}{d\lambda} = \left[\frac{dI_{z0}}{d\lambda}, \frac{dI_{z1}}{d\lambda}, \dots, \frac{dI_{zl}}{d\lambda} \right]^T. \quad (31c)$$

The integral of (27) reads

$$\begin{aligned} & \int_S G(\mathbf{r}, \mathbf{r}') F_3^{(2)}(\mathbf{r}') (-Z_e) dS \\ &= \int_S G(\mathbf{r}, \mathbf{r}') (-Z_e) I_{z0} \frac{d\delta(\mathbf{r}' - \mathbf{r}_0)}{d\mathbf{r}_j} \\ & \quad + \dots + G(\mathbf{r}, \mathbf{r}') (-Z_e) I_{zl} \frac{d\delta(\mathbf{r}' - \mathbf{r}_l)}{d\mathbf{r}_j} dS. \end{aligned} \quad (32)$$

To compute (32), we apply (29). Although we cannot directly use this property, because the variable of differentiation and integration can be the same, however, by means of a change of variable, the problem can be circumvented. This is done by multiplying and dividing by $d(\mathbf{r}' - \mathbf{r}_j)$. Considering for simplicity only the first term, we obtain

$$\begin{aligned} & \int_{-\infty}^{+\infty} \frac{d\delta(\mathbf{r}' - \mathbf{r}_0)}{d\mathbf{r}_j} G(\mathbf{r}, \mathbf{r}') d\mathbf{r}' \\ &= \int_{-\infty}^{+\infty} \frac{d\delta(\mathbf{r}' - \mathbf{r}_0)}{d(\mathbf{r}' - \mathbf{r}_j)} \frac{d(\mathbf{r}' - \mathbf{r}_j)}{d\mathbf{r}_j} G(\mathbf{r}, \mathbf{r}') d\mathbf{r}' \\ &= - \int_{-\infty}^{+\infty} \frac{d\delta(\mathbf{r}' - \mathbf{r}_0)}{d\mathbf{r}'} G(\mathbf{r}, \mathbf{r}') d\mathbf{r}' \\ &= \left. \frac{dG(\mathbf{r}, \mathbf{r}_0)}{d\mathbf{r}'} \right|_{\mathbf{r}'=\mathbf{r}_j} = \frac{dG(\mathbf{r}, \mathbf{r}_0)}{d\mathbf{r}_j}. \end{aligned} \quad (33)$$

Thus, the sensitivity reads

$$\hat{v}(\mathbf{r}; \lambda) = \tilde{G}(\mathbf{r}) (-Z_e) \frac{d\tilde{I}_z}{d\lambda} + \frac{d\tilde{G}(\mathbf{r})}{d\lambda} (-Z_e) \tilde{I}_z \quad (34)$$

where

$$\frac{d\tilde{G}(\mathbf{r})}{d\lambda} = \left[\frac{dG(\mathbf{r}, \mathbf{r}_0)}{d\lambda}, \frac{dG(\mathbf{r}, \mathbf{r}_1)}{d\lambda}, \dots, \frac{dG(\mathbf{r}, \mathbf{r}_l)}{d\lambda} \right]. \quad (35)$$

B. Geometrical or Electrical Parameter

The voltage sensitivity with respect to a geometrical or electrical parameter can be treated in a different way. In this case, the γ^2 and Z_e parameter could be dependent on the λ parameter and the values of F_1 and F_2 could be different from zero.

First we consider the F_1 term from (23). We can solve

$$\int_S G(\mathbf{r}, \mathbf{r}') F_1(\mathbf{r}') dS \quad (36)$$

where $v(\mathbf{r}')$ can be considered as the solution of the Sturm–Liouville problem, with the same equivalent current vector J_z as in [9]. So

$$v(\mathbf{r}') = \int_S G(\mathbf{r}', \mathbf{r}'') (-Z_e) J_z(\mathbf{r}'') dS. \quad (37)$$

For the Dirac delta function property (28), if we consider $h(z'') = G(\mathbf{r}', \mathbf{r}'')$, the integral of (37) becomes

$$\begin{aligned} v(\mathbf{r}') &= \cdot [G(\mathbf{r}', \mathbf{r}_0) (-Z_e) I_{z0} \\ & \quad + G(\mathbf{r}', \mathbf{r}_1) (-Z_e) I_{z1} + \dots \\ & \quad + G(\mathbf{r}', \mathbf{r}_l) (-Z_e) I_{zl}] \\ &= \tilde{G}(\mathbf{r}') (-Z_e) \tilde{I}_z. \end{aligned} \quad (38)$$

Since the terms $d\gamma^2/d\lambda$, $-Z_e$ and \tilde{I}_z do not depend on \mathbf{r}' , substituting (38) into (36), we obtain

$$\begin{aligned} & \int_S G(\mathbf{r}, \mathbf{r}') F_1(\mathbf{r}') dS \\ &= \int_S G(\mathbf{r}, \mathbf{r}') \cdot \frac{d\gamma^2}{d\lambda} (-Z_e) (\tilde{G}(\mathbf{r}') \tilde{I}_z) \\ &= \frac{d\gamma^2}{d\lambda} (-Z_e) \int_S G(\mathbf{r}, \mathbf{r}') \tilde{G}(\mathbf{r}') dS \cdot \tilde{I}_z. \end{aligned} \quad (39)$$

We also notice that the \tilde{I}_z term, due to the property of the matrix product, can be placed on the right side of the integral. Now we can consider the integral (39)

$$\int_S G(\mathbf{r}, \mathbf{r}') \tilde{G}(\mathbf{r}') dS = \Gamma(\mathbf{r}). \quad (40)$$

For the particular structure of $\tilde{G}(\mathbf{r}')$ in (31a), the result of the integral will be a vector of the form

$$\Gamma(\mathbf{r}) = [\Gamma_0(\mathbf{r}), \Gamma_1(\mathbf{r}), \dots, \Gamma_l(\mathbf{r})] \quad (41)$$

where

$$\Gamma_i(\mathbf{r}) = \int_S G(\mathbf{r}, \mathbf{r}') G(\mathbf{r}', \mathbf{r}_i) dS. \quad (42)$$

For the sake of simplicity we can consider only the case of the first term ($\Gamma_0(\mathbf{r})$), because the procedure can be extended also to the remaining terms. Thus, recalling (22b), we can write

$$\begin{aligned} \Gamma_0(\mathbf{r}) &= \int_S G(\mathbf{r}, \mathbf{r}') G(\mathbf{r}', \mathbf{r}_0) dS \\ &= \int_S \sum_{m=0}^{\infty} \sum_{n=0}^{\infty} \Phi_{mn}(s) N_{mn}(\mathbf{r}) N_{mn}(\mathbf{r}') \\ & \quad \cdot \sum_{m'=0}^{\infty} \sum_{n'=0}^{\infty} \Phi_{m'n'}(s) N_{m'n'}(\mathbf{r}') N_{m'n'}(\mathbf{r}_0) dS. \end{aligned} \quad (43)$$

The eigenfunctions $N_{mn}(\cdot)$ and $N_{m'n'}(\cdot)$ constitute two orthonormal bases and, therefore, the integral of their product is different from zero only if $(m, n) = (m', n')$. In this way, we can consider only one double sum

$$\begin{aligned} \Gamma_0(\mathbf{r}) &= \sum_{m=0}^{\infty} \sum_{n=0}^{\infty} \Phi_{mn}(s)^2 N_{mn}(\mathbf{r}) N_{mn}(\mathbf{r}_0) \\ & \quad \cdot \int_S N_{mn}(\mathbf{r}') N_{mn}(\mathbf{r}') dS \\ &= \sum_{m=0}^{\infty} \sum_{n=0}^{\infty} \Phi_{mn}(s)^2 N_{mn}(\mathbf{r}) N_{mn}(\mathbf{r}_0) \cdot \xi_{mn} \end{aligned} \quad (44)$$

where

$$\xi_{mn} = \int_S N_{mn}(\mathbf{r}') N_{mn}(\mathbf{r}') dS. \quad (45)$$

Expanding (45), we obtain

$$\xi_{mn} = \int_0^a \int_0^b N_{mn}(x', y') N_{mn}(x', y') dx' dy'$$

$$= K \cdot \int_0^a \int_0^b \cos^2 \left(\frac{m\pi x'}{a} \right) \cdot \cos^2 \left(\frac{n\pi y'}{b} \right) dx' dy' \quad (46)$$

where

$$K = C_m C_n. \quad (47)$$

We can distinguish the case of the pair $(m, n) = (0, 0)$ from the case $(m, n) \neq (0, 0)$. In the first case the argument of integral (46) will be unity and therefore the result can be written as

$$\xi_{00} = K \cdot ab. \quad (48)$$

Otherwise, the solution of (46) will be

$$\begin{aligned} \xi_{mn} &= K \cdot \int_0^a \cos^2 \left(\frac{m\pi x'}{a} \right) dx' \cdot \int_0^b \cos^2 \left(\frac{n\pi y'}{b} \right) dy' \\ &= K \cdot \left[\frac{1}{2} \left(x' + \frac{a}{m\pi} \cos \left(\frac{m\pi x'}{a} \right) \sin \left(\frac{m\pi x'}{a} \right) \right) \right]_0^a \\ &\quad \cdot \left[\frac{1}{2} \left(y' + \frac{b}{n\pi} \cos \left(\frac{n\pi y'}{b} \right) \sin \left(\frac{n\pi y'}{b} \right) \right) \right]_0^b. \quad (49) \end{aligned}$$

In the case m (n) is equal to zero, we can only consider the second (first) part of (49). Hence, the result reads

$$\begin{aligned} \xi_{m0} &= K \cdot \frac{1}{2} ab \\ \xi_{0n} &= K \cdot \frac{1}{2} ab \\ \xi_{mn} &= K \cdot \frac{1}{4} ab. \quad (50) \end{aligned}$$

The second term $F_2(\mathbf{r}')$ reads

$$\int_S G(\mathbf{r}, \mathbf{r}') F_2(\mathbf{r}') dS = \int_S G(\mathbf{r}, \mathbf{r}') \left(-\frac{dZ_e}{d\lambda} \right) J_z dS. \quad (51)$$

Again, due to the Dirac delta function property (28), the result of the integral becomes

$$\begin{aligned} &\int_S G(\mathbf{r}, \mathbf{r}') F_2(\mathbf{r}') dS \\ &= \left[G(\mathbf{r}, \mathbf{r}_0) \left(-\frac{dZ_e}{d\lambda} \right) I_{z0} \right. \\ &\quad \left. + G(\mathbf{r}, \mathbf{r}_1) \left(-\frac{dZ_e}{d\lambda} \right) I_{z1} + \dots \right. \\ &\quad \left. + G(\mathbf{r}, \mathbf{r}_l) \left(-\frac{dZ_e}{d\lambda} \right) I_{zl} \right] \\ &= \tilde{G}(\mathbf{z}) \left(-\frac{dZ_e}{d\lambda} \right) \tilde{I}_z. \quad (52) \end{aligned}$$

We can notice that, if Z_e does not depend on λ , the $F_2(\mathbf{r}')$ term can be neglected.

For the third term $F_3(\mathbf{r})$, the derivative of $\delta(\mathbf{r}' - \mathbf{r}_i)$ is equal to zero because the function does not depend on λ unlike as (25). We can write

$$F_3(\mathbf{r}') = -Z_e \frac{dJ_z}{d\lambda}$$

$$= -Z_e \left[\frac{dI_{z0}}{d\lambda} \delta(\mathbf{r}' - \mathbf{r}_0) + \frac{dI_{z1}}{d\lambda} \delta(\mathbf{r}' - \mathbf{r}_1) + \dots + \frac{dI_{zl}}{d\lambda} \delta(\mathbf{r}' - \mathbf{r}_l) \right]. \quad (53)$$

Applying the property (28) we obtain

$$\begin{aligned} &\int_S G(\mathbf{r}, \mathbf{r}') F_3(\mathbf{r}') dS \\ &= \int_S G(\mathbf{r}, \mathbf{r}') (-Z_e) \frac{dJ_z}{d\lambda} \\ &= -Z_e \left[\frac{dI_{z0}}{d\lambda} G(\mathbf{r}, \mathbf{r}_0) + \frac{dI_{z1}}{d\lambda} G(\mathbf{r}, \mathbf{r}_1) + \dots \right. \\ &\quad \left. + \frac{dI_{zl}}{d\lambda} G(\mathbf{r}, \mathbf{r}_l) \right] \\ &= \tilde{G}(\mathbf{r}) (-Z_e) \frac{d\tilde{I}_z}{d\lambda}. \quad (54) \end{aligned}$$

Finally, the sensitivity reads

$$\begin{aligned} \hat{v}(\mathbf{r}; \lambda) &= -\frac{d\gamma^2}{d\lambda} Z_e \Gamma(\mathbf{r}) \tilde{I}_z + \tilde{G}(\mathbf{r}) \\ &\quad \times \left(-\frac{dZ_e}{d\lambda} \right) \tilde{I}_z + \tilde{G}(\mathbf{r}) (-Z_e) \frac{d\tilde{I}_z}{d\lambda}. \quad (55) \end{aligned}$$

IV. COMPUTATION OF DERIVATIVES

To compute the voltage sensitivity in (34) and (55) we need to know the expression of several derivatives depending on the sensitivity parameter.

A. Port Positions

The derivatives involved in (34) are the derivative of the port current vector \tilde{I}_z and the derivative of the Green's function $G(\mathbf{r}, \mathbf{r}_j)$ function with respect to the \mathbf{r}_j parameter.

The derivative with respect to $\lambda = \mathbf{r}_j$ of the $G(\mathbf{r}, \mathbf{r}')$ function can be analytically computed. In particular, recalling (22b), we can distinguish the case of the self and the mutual Green's function in this way

$$\begin{aligned} \frac{d}{d\mathbf{r}_j} G(\mathbf{r}_j, \mathbf{r}_j) &= \sum_{m=0}^{\infty} \sum_{n=0}^{\infty} \Phi_{mn}(s) \\ &\quad \times \frac{d}{d\mathbf{r}_j} [N_{mn}(\mathbf{r}_j) N_{mn}(\mathbf{r}_j)] \\ \frac{d}{d\mathbf{r}_j} G(\mathbf{r}_j, \mathbf{r}_i) &= \sum_{m=0}^{\infty} \sum_{n=0}^{\infty} \Phi_{mn}(s) N_{mn}(\mathbf{r}_i) \\ &\quad \times \frac{d}{d\mathbf{r}_j} [N_{mn}(\mathbf{r}_j)]. \quad (56) \end{aligned}$$

Otherwise, if the Green's function $G(\mathbf{r}, \mathbf{r}')$ does not depend on \mathbf{r}_j , its derivative is equal to zero

$$\frac{d}{d\mathbf{r}_j} G(\mathbf{r}_i, \mathbf{r}_k) = 0 \quad i, k \neq j. \quad (57)$$

The port voltages can be expressed in terms of the port currents as

$$[\tilde{V}] = [Z] \cdot [\tilde{I}_z] \quad (58)$$

where $[\tilde{V}]$ represents the vector of the port voltages

$$[\tilde{V}] = [V_0 \quad V_1 \quad \dots \quad V_l]^T \quad (59)$$

and the impedance matrix $[Z]$ can be expressed in terms of the Green's functions

$$[Z] = \begin{bmatrix} G(\mathbf{r}_0, \mathbf{r}_0)(-Z_e) & \dots & G(\mathbf{r}_0, \mathbf{r}_l)(-Z_e) \\ G(\mathbf{r}_1, \mathbf{r}_0)(-Z_e) & \dots & G(\mathbf{r}_1, \mathbf{r}_l)(-Z_e) \\ \vdots & \ddots & \vdots \\ G(\mathbf{r}_l, \mathbf{r}_0)(-Z_e) & \dots & G(\mathbf{r}_l, \mathbf{r}_l)(-Z_e) \end{bmatrix}. \quad (60)$$

In addition, boundary condition have to be enforced at the electrical ports. If linear terminations are considered, they can be written in a matrix form as

$$[\tilde{V}] = [V_S] - [Z_0] \cdot [\tilde{I}_z] \quad (61)$$

where the input voltage source vector $[V_S]$ and the termination impedance matrix $[Z_0]$ are

$$[\tilde{V}_S] = [V_{S0} \quad V_{S1} \quad \dots \quad V_{Sl}]^T$$

$$[Z_0] = \begin{bmatrix} Z_{0,1} & 0 & \dots & 0 \\ 0 & Z_{0,1} & \dots & 0 \\ \vdots & \vdots & \ddots & \vdots \\ 0 & 0 & \dots & Z_{0,l} \end{bmatrix}. \quad (62)$$

After trivial matrix manipulations, port currents can be expressed directly in terms of the source voltages as

$$[\tilde{I}_z] = ([Z_0] + [Z])^{-1} [V_S]. \quad (63)$$

Now we are ready to compute the derivative of the port current vector $[\tilde{I}_z]$ (63) as

$$\frac{d}{d\lambda} [\tilde{I}_z] = \frac{d}{d\lambda} ([Z_0] + [Z])^{-1} [V_S]. \quad (64)$$

Such a computation can be more efficiently performed through the use of the following theorem

Theorem 1: Suppose \mathbf{A} is a square matrix depending on a real parameter λ taking values in an open set $I \subseteq \mathfrak{R}$. Further, suppose all component functions in \mathbf{A} are differentiable, and $\mathbf{A}(\lambda)$ is differentiable for all λ . Then, in I , we have

$$\frac{d\mathbf{A}^{-1}}{d\lambda} = -\mathbf{A}^{-1} \frac{d\mathbf{A}}{d\lambda} \mathbf{A}^{-1}$$

where $d/d\lambda$ is the derivative. Hence, (64) becomes

$$\frac{d}{d\lambda} [\tilde{I}_z] = ([Z_0] + [Z])^{-1} \cdot \frac{d}{d\lambda} [Z] \cdot ([Z_0] + [Z])^{-1} [V_S]. \quad (65)$$

The derivative of matrix $[Z]$ can now be computed from (60) taking (57) and (56) into account and by recalling that Z_s is independent of r_j .

B. Geometrical or Electrical Parameter

Equation (55) shows the derivative for the sensitivity applied to geometrical or electrical parameter. The derivative of γ^2 and Z_e depends on the choice of the λ parameter. Otherwise the derivative of I_z can be computed as in (65). The only difference is that the derivative of the Green's function G has to be computed in different form as in (56) and (57) and also in this case depends on the choice of the λ parameter.

V. TIME-DOMAIN MODEL

From (58), the port voltage can be expressed in terms of the port current, and the sensitivity applied at (58) reads

$$[\hat{V}] = [Z][\hat{I}] + [\hat{Z}][I]. \quad (66)$$

Impedance matrix $[Z]$ entries can be rewritten as [7]

$$Z_{ij}(s) = \sum_{m=0}^{\infty} \sum_{n=0}^{\infty} \frac{Z_e \cdot N_{mn}(\mathbf{r}_i) N_{mn}(\mathbf{r}_j)}{(k_{mn}^2 - k^2) ab}. \quad (67)$$

The rational structure of (67) is well suited for a pole/residue identification, leading to

$$Z_{ij}(s) = \sum_{k=1}^{\infty} \frac{R_{ij,k}}{s - p_k} \quad (68)$$

which can be easily converted to a state-space model [23]

$$\begin{aligned} \dot{\mathbf{x}}_1(t) &= \mathbf{A}_1 \mathbf{x}_1(t) + \mathbf{B}_1 \hat{\mathbf{i}}(t) \\ \hat{\mathbf{v}}_1(t) &= \mathbf{C}_1 \mathbf{x}_1(t). \end{aligned} \quad (69)$$

Furthermore, the impedance matrix sensitivity $[\hat{Z}]$ can be written as

$$[\hat{Z}] = -\frac{d\gamma^2}{d\lambda} Z_e \Gamma + \tilde{G} \left(-\frac{dZ_e}{d\lambda} \right) \quad (70)$$

where matrices Γ and \tilde{G} are obtained by computing (41) and (31a) at the electrical ports.

Since both the two contributions to the impedance sensitivity have a rational form, they admit a state-space realization

$$\begin{aligned} \dot{\mathbf{x}}_2(t) &= \mathbf{A}_2 \mathbf{x}_2(t) + \mathbf{B}_2 \hat{\mathbf{i}}(t) \\ \hat{\mathbf{v}}_2(t) &= \mathbf{C}_2 \mathbf{x}_2(t) \end{aligned} \quad (71)$$

where $\hat{\mathbf{i}}(t) = [\hat{\mathbf{i}}_1(t) \quad \hat{\mathbf{i}}_2(t)]^T$, $\hat{\mathbf{i}}(t) = [\hat{\mathbf{i}}_1(t) \quad \hat{\mathbf{i}}_2(t)]^T$. In addition, (58) admits a space-state realization \mathbf{A} , \mathbf{B} , \mathbf{C} which coincides with \mathbf{A}_1 , \mathbf{B}_1 , \mathbf{C}_1 (69)

$$\begin{aligned} \dot{\mathbf{x}}(t) &= \mathbf{A} \mathbf{x}(t) + \mathbf{B} \hat{\mathbf{i}}(t) \\ \mathbf{v}(t) &= \mathbf{C} \mathbf{x}(t). \end{aligned} \quad (72)$$

The voltage sensitivity can be finally expressed as

$$\hat{\mathbf{v}}(t) = \hat{\mathbf{v}}_1(t) + \hat{\mathbf{v}}_2(t) = \mathbf{C}_1 \mathbf{x}_1(t) + \mathbf{C}_2 \mathbf{x}_2(t) \quad (73)$$

and a global state-space model can be generated as

$$\begin{bmatrix} \dot{\mathbf{x}}_1(t) \\ \dot{\mathbf{x}}_2(t) \\ \dot{\mathbf{x}}(t) \end{bmatrix} = \begin{bmatrix} \mathbf{A}_1 & 0 & 0 \\ 0 & \mathbf{A}_2 & 0 \\ 0 & 0 & \mathbf{A} \end{bmatrix} \cdot \begin{bmatrix} \mathbf{x}_1(t) \\ \mathbf{x}_2(t) \\ \mathbf{x}(t) \end{bmatrix} + \begin{bmatrix} \mathbf{B}_1 & 0 \\ 0 & \mathbf{B}_2 \\ \mathbf{B} & 0 \end{bmatrix} \cdot \begin{bmatrix} \hat{\mathbf{i}}(t) \\ \hat{\mathbf{i}}(t) \end{bmatrix} \quad (74)$$

$$\begin{bmatrix} \mathbf{v}(t) \\ \hat{\mathbf{v}}(t) \end{bmatrix} = \begin{bmatrix} 0 & 0 & \mathbf{C} \\ \mathbf{C}_1 & \mathbf{C}_2 & 0 \end{bmatrix} \cdot \begin{bmatrix} \mathbf{x}_1(t) \\ \mathbf{x}_2(t) \\ \mathbf{x}(t) \end{bmatrix}. \quad (75)$$

A. Terminations

Port terminations are assumed to be described by current sources and voltage driven lumped elements such that the following equation holds:

$$\dot{\mathbf{i}}(t) = \mathbf{i}_s(t) - \mathbf{G}\mathbf{v}(t) - \mathbf{C}\frac{d\mathbf{v}(t)}{dt} \quad (76)$$

where $\mathbf{v}(t)$ and $\mathbf{i}(t)$ are the vectors of the unknown port voltages and currents, $\mathbf{i}_s(t)$ represents the current source vector, matrices \mathbf{G} , \mathbf{C} describe linear resistive and capacitive lumped elements, respectively. The sensitivity of the terminations with respect to a parameter λ can be obtained using (76) as

$$\hat{\mathbf{i}}(t) = -\mathbf{G}\hat{\mathbf{v}}(t) - \mathbf{C}\frac{d\hat{\mathbf{v}}(t)}{dt}. \quad (77)$$

Substituting (73) into (77), we obtain

$$\hat{\mathbf{i}}(t) = -\mathbf{G}[\mathbf{C}_1\mathbf{x}_1(t) + \mathbf{C}_2\mathbf{x}_2(t)] - \mathbf{C}[\mathbf{C}_1\dot{\mathbf{x}}_1(t) + \mathbf{C}_2\dot{\mathbf{x}}_2(t)]. \quad (78)$$

In order to compute (76) and (78), we need to evaluate the port voltages and currents, $\mathbf{v}(t)$ and $\mathbf{i}(t)$ respectively. They can be computed from (58) which admits a space-state realization. Once $\mathbf{v}(t)$ and $\mathbf{i}(t)$ are computed through (72) and the corresponding terminal conditions (76), we can solve the system of ordinary differential equations (ODEs) (69) and (71) along with the terminations (78) where the input vector is represented by the port currents $\mathbf{i}(t)$. To this aim, we can substitute (78) into (71)

$$\begin{aligned} [\mathbf{I} + \mathbf{B}_2\mathbf{C}\mathbf{C}_2]\dot{\mathbf{x}}_2(t) &= [\mathbf{A}_2 - \mathbf{B}_2\mathbf{G}\mathbf{C}_2] \cdot \mathbf{x}_2(t) \\ &\quad - [\mathbf{B}_2\mathbf{G}\mathbf{C}_1]\mathbf{x}_1(t) + \mathbf{B}_2\mathbf{C}\mathbf{C}_1\dot{\mathbf{x}}_1(t). \end{aligned} \quad (79)$$

The expression of $\dot{\mathbf{x}}_1(t)$ can be obtained directly from (69). Substituting (69) into (79), we obtain

$$\begin{aligned} [\mathbf{I} + \mathbf{B}_2\mathbf{C}\mathbf{C}_2]\dot{\mathbf{x}}_2(t) &= [\mathbf{A}_2 - \mathbf{B}_2\mathbf{G}\mathbf{C}_2] \cdot \mathbf{x}_2(t) \\ &\quad - [\mathbf{B}_2\mathbf{G}\mathbf{C}_1 + \mathbf{B}_2\mathbf{C}\mathbf{C}_1\mathbf{A}_1]\mathbf{x}_1(t) - \mathbf{B}_2\mathbf{C}\mathbf{C}_1\mathbf{B}_1\dot{\mathbf{i}}(t). \end{aligned} \quad (80)$$

The solution of (80) requires the vector of the unknown $\mathbf{x}_1(t)$, already computed in (69), and the port voltage and current, $\mathbf{v}(t)$ and $\mathbf{i}(t)$, respectively, already evaluated by (72) and (76) and, therefore, it can be easily carried out.

Remark 2: The presented technique is based on the closed-form Green's function for voltages via planar-circuit approach for a single power-bus pair [5], [6]. The extension of such an approach to multiple plains can be obtained as described in

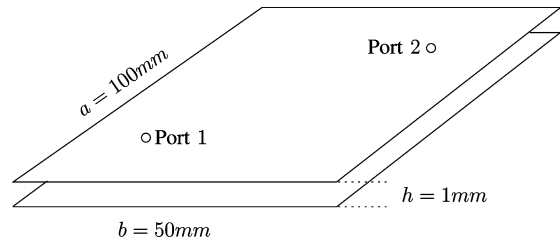


Fig. 2. Test board geometry.

[24]. The sensitivity analysis of multiple plains structures can be based on the proposed technique and will be investigated in forthcoming reports.

VI. NUMERICAL RESULTS

In this section we propose both frequency and time-domain analysis in order to verify the validity and strength of the proposed approach. The frequency-domain results are validated through comparison with the perturbative approach computing the voltage sensitivity as

$$\widehat{V}(j\omega; \lambda) = \frac{[V(j\omega; \lambda + \Delta\lambda)] - [V(j\omega; \lambda)]}{\Delta\lambda} \quad (81)$$

where $\Delta\lambda$ represents the perturbation. Time-domain values are compared with those obtained by using the frequency-domain data via the inverse fast Fourier transform (IFFT).

A. Frequency-Domain

We applied the proposed approaches to the power-bus structure shown in Fig. 2. The board dimensions are $a = 100$ mm (length), $b = 50$ mm (width), $h = 1$ mm thickness. On the board are placed two ports with coordinates: port 1 (20 mm, 20 mm), port 2 (70 mm, 40 mm). The dielectric relative permittivity is $\epsilon_r = 3.4$. The number of the modes used for computation of the Green's function is set to 10 along both the x and y axes and the frequency range is [1 MHz–20 GHz].

1) *Port Positions:* First we consider the case of port variation. In particular, we compute the sensitivity on port 1 and port 2 when a variation along x of port 2 is affected. The input to this circuit through the port 1 is a 1 ns voltage pulse with 300 ps rise and fall times. We compare the sensitivity computed as (34) and the perturbative approach. Both the ports are terminated in 50Ω resistances. The magnitude and phase sensitivity spectra are shown in Figs. 3 and 4 for port 1 and 2, respectively. As it clearly seen, a satisfactory agreement is obtained over the entire frequency range.

2) *Thickness of the Dielectric Substrate:* In the second test, the voltage sensitivity is computed with respect to the thickness of the dielectric substrate, $\lambda = h$. It is to be noted that, since the Green's function does not depend on $\lambda = h$, the derivative of the $G_{i,j}$ functions are equal to zero for each $i, j = 0, \dots, l$. The input is the same of the previous test as well as the terminations. The comparison of the sensitivities at the port 1 and 2 are computed by (55) and the perturbative approach and are shown in Figs. 5 and 6.

In both the tests a satisfactory agreement is achieved.

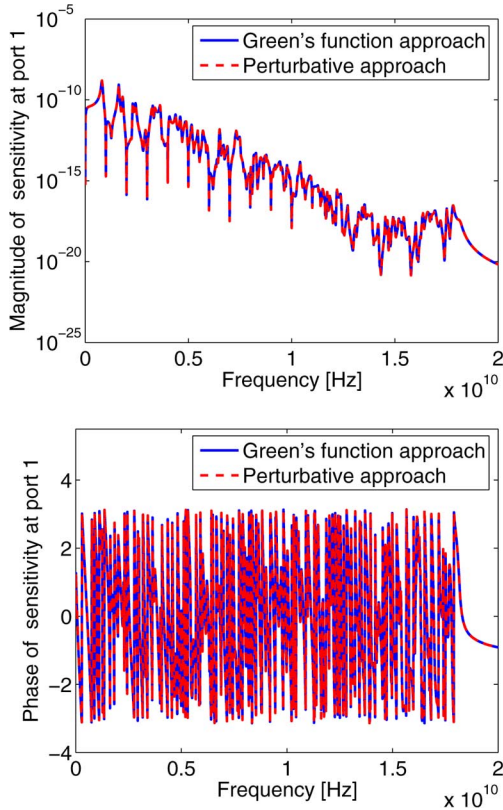


Fig. 3. Port position—magnitude and phase spectra at port 1.

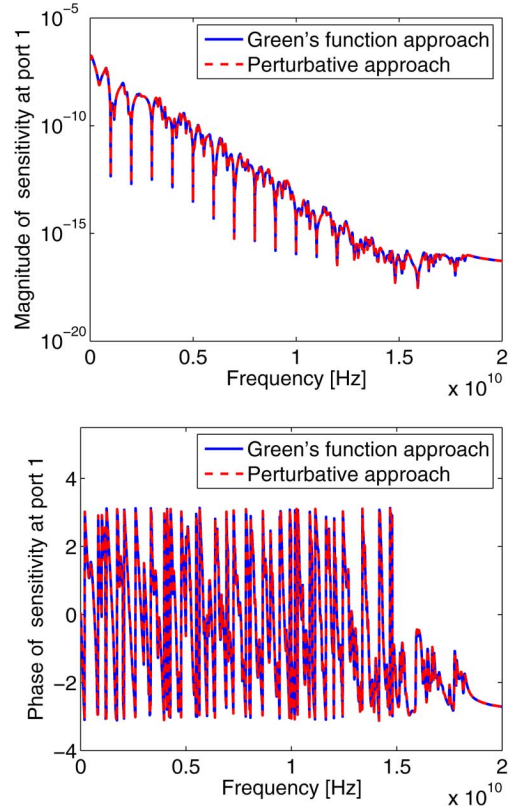


Fig. 5. Thickness of the dielectric substrate—magnitude and phase spectra at port 1.

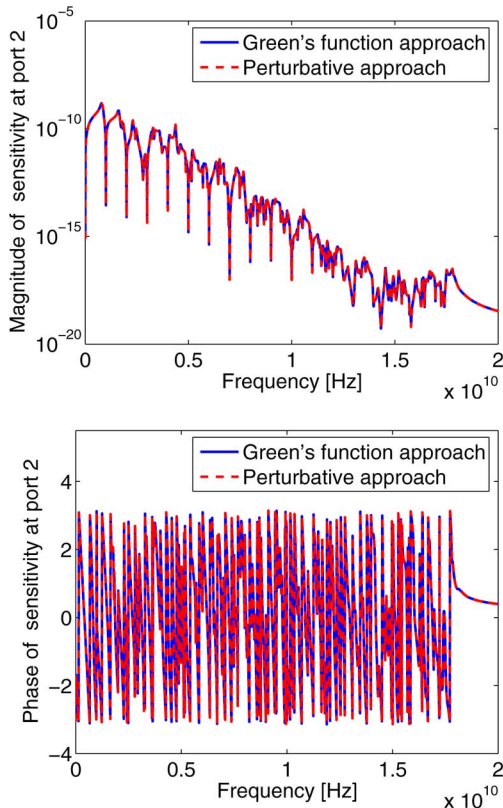


Fig. 4. Port position—magnitude and phase spectra at port 2.

B. Time-Domain Results

The time-domain analysis of the same board in Fig. 2 has been carried out. As in the frequency-domain analysis, both thickness of dielectric substrate and port position have been considered for the sensitivity analysis. The input at the port 1 is represented by a 1 ns voltage pulse with amplitude of 1 V, initial delay of 1 ns and 200 ps rise and fall times. The relative dielectric permittivity is $\epsilon_r = 3.4$. The series form has been limited to 10 modes along both the x and y axes. As before, the ports are terminated in 50Ω resistances. The analysis is extended to 60 ns and the integration step is 2 ps. We compare the integration of the space state model proposed and the inverse fast Fourier transform (IFFT) of the frequency sensitivity computed as explained in Section VI-A.

The voltage sensitivity with respect to the port position is shown in Fig. 7, while the voltage sensitivity with respect to the thickness of dielectric substrate is shown, respectively, in Fig. 8. Table I shows the a comparison of computational cost using the proposed approach versus the IFFT-based method, assuming $3 \cdot 10^4$ time samples and 3600 frequency samples. The cpu-time saving is about 74% for a single parameter run and can be even larger when multiparameter sensitivity is considered in the framework of an optimization process.

VII. CONCLUSION

In this paper, a new methodology for both time and frequency domain sensitivity analysis of power-bus has been presented. Relying on the fact the propagation of voltages and the corresponding sensitivities with respect to a generic parameter λ obey

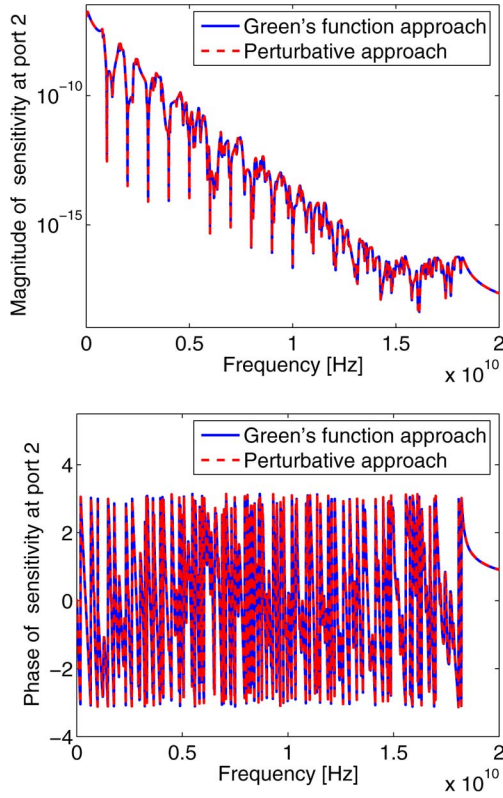


Fig. 6. Thickness of the dielectric substrate—magnitude and phase spectra at port 2.

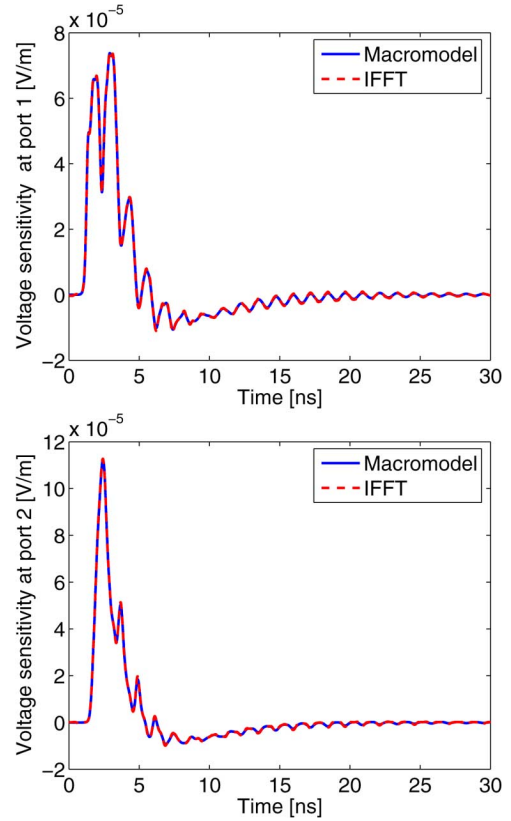


Fig. 8. Thickness of the dielectric substrate—time sensitivity analysis at port 1 and 2.

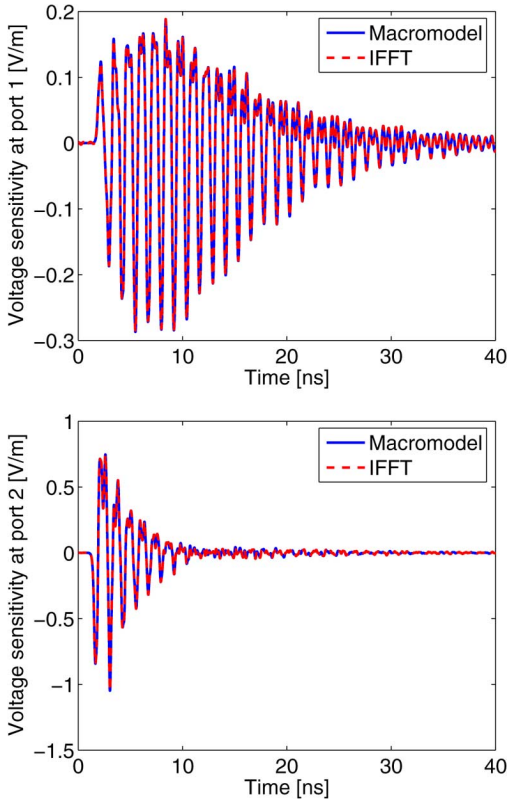


Fig. 7. Port position—time sensitivity analysis at port 1 and 2.

to the same differential equation, the 2-D TM Green's function

TABLE I
COMPUTATIONAL COST: PROPOSED VERSUS IFFT

	Proposed	IFFT
Cpu-time [s]	81	309

is used to compute both voltage and sensitivities as convolution integral between the Green's function itself and a forcing term which can be analytically computed. Furthermore, since the model inherits the rational form from the Green's function, the time-domain macromodel in space-state form is easily generated by using standard realization techniques. Hence, the proposed method provides a systematic approach to frequency and time-domain sensitivity analysis of power-bus structures. The validation of the proposed method is carried out by comparing the numerical results with those obtained using standard approaches in both the frequency and time-domain, confirming its reliability and robustness.

REFERENCES

- [1] X.-P. Yang and Z.-F. Li, "An efficient time-domain macromodel for power/ground bounce analysis," *Microw. Opt. Technol. Lett.*, vol. 28, no. 2, pp. 224–226, Feb. 2001.
- [2] C.-C. Huang, "Circuit modeling of power/ground plane structures for printed circuit boards," *Microw. Opt. Technol. Lett.*, vol. 47, no. 1, pp. 97–99, Oct. 2005.
- [3] K. S. Yee, "Numerical solution of initial boundary value problems involving Maxwell's equations in isotropic media," *IEEE Trans. Antennas Propagat.*, vol. AP-14, no. 3, pp. 302–307, May 1966.
- [4] A. E. Ruehli, P. A. Brennan, and Techniques, "Efficient capacitance calculations for three-dimensional multiconductor systems," *IEEE Trans. Microw. Theory Tech.*, vol. 21, no. 2, pp. 76–82, Feb. 1973.

- [5] G. T. Lei, R. W. Techentin, P. R. Hayes, D. J. Schwab, and B. K. Gilbert, "Wave model solution to the ground/power plane noise," *IEEE Trans. Instrum. Meas.*, vol. 44, no. 2, pp. 300–303, May 1995.
- [6] G. T. Lei, R. W. Techentin, and B. K. Gilbert, "High-frequency characterization of power/ground-plane structures," *IEEE Trans. Microw. Theory Tech.*, vol. 47, no. 5, pp. 562–569, May 1999.
- [7] G. Antonini, "A low frequency accurate cavity model for transient analysis of power-ground structures," *IEEE Trans. Electromagn. Compat.*, vol. 50, no. 1, pp. 138–148, Feb. 2008.
- [8] T. Okoshi, Y. Uehara, and T. Takeuchi, "The segmentation method—an approach to the analysis of microwave planar circuits," *IEEE Trans. Microw. Theory Tech.*, vol. 24, no. 10, pp. 662–668, Oct. 1976.
- [9] R. Sorrentino, "Planar circuits, waveguide models and segmentation method," *IEEE Trans. Microw. Theory Tech.*, vol. 33, no. 10, pp. 1057–1066, Oct. 1985.
- [10] Z. L. Wang, O. Wada, Y. Toyota, and R. Koga, "Modeling of gapped power bus structures for isolation using cavity modes and segmentation," *IEEE Trans. Electromagn. Compat.*, vol. 47, no. 2, pp. 210–218, May 2005.
- [11] J. Mao, C. Wang, L. Zhang, R. E. DuBroff, J. L. Drewniak, A. Orlandi, and G. Antonini, "An efficient analysis method for the power-bus impedance," presented at the Int. Symp. Electromagnetic Compatibility, Eindhoven, The Netherlands, Sep. 2004.
- [12] W. F. Richards and Y. T. Lo, "Theoretical and experimental investigation of a microstrip radiation with multiple lumped linear loads," *Electromagn.*, vol. 3, no. 3-4, pp. 371–385, 1983.
- [13] A. Benalla and K. C. Gupta, "Faster computation of Z-matrices for rectangular segments in planar microstrip circuits," *IEEE Trans. Microw. Theory Tech.*, vol. 34, no. 6, pp. 733–736, Jun. 1986.
- [14] Z. L. Wang, O. Wada, Y. Toyota, and R. Koga, "Convergence acceleration and accuracy improvement in power bus impedance calculation with a fast algorithm using cavity modes," *IEEE Trans. Electromagn. Compat.*, vol. 47, no. 1, pp. 2–9, Feb. 2005.
- [15] P. Liu and Z.-F. Li, "An efficient method for calculating bounces in the irregular power/ground plane structure with holes in high-speed PCBs," *IEEE Trans. Electromagn. Compat.*, vol. 47, no. 4, pp. 889–898, Nov. 2005.
- [16] L. C. Fung, S. W. Leung, L. Wan, Y. M. Siu, and K. H. Chen, "Investigation of ground bounce effect on PCBs," *Microw. Opt. Technol. Lett.*, vol. 32, no. 4, pp. 259–264, Feb. 2002.
- [17] A. E. Engin, K. Bharath, M. Swaminathan, M. Cases, B. Mutmury, N. Pham, D. N. d. Araujo, and E. Matoglu, "Finite-difference modeling of noise coupling between power/ground planes in multilayered packages and boards," presented at the Proc. Electron. Compon. Technol. Conf., San Diego, CA, May 2006.
- [18] S. Sun, D. Pommerenke, J. Drewniak, K. Xiao, S.-T. Chen, and T.-L. Wu, "Characterizing package/PCB PDN interactions from a full-wave finite difference formulation," in *Proc. IEEE Int. Symp. Electromagn. Compatibil.*, Portland, OR, Aug. 2006, pp. 550–555.
- [19] R. L. Chen, J. Chen, T. H. Hubing, and W. Shi, "Analytical model for the rectangular power-ground structure including radiation loss," *IEEE Trans. Electromagn. Compat.*, vol. 47, no. 1, pp. 10–16, Feb. 2005.
- [20] H.-W. Woo and T. H. Hubing, "A closed-form expression for estimating radiated emissions from the power planes in a populated printed circuit board," *IEEE Trans. Electromagn. Compat.*, vol. 48, no. 1, pp. 74–81, Feb. 2006.
- [21] T. Okoshi, *Planar Circuits for Microwaves and Lightwaves*. Berlin, Germany: Springer-Verlag, 1985.
- [22] J. V. Bladel, *Singular Electromagnetic Fields and Sources*. Oxford, U.K.: Clarendon, 1991.
- [23] C.-T. Chen, *Linear System Theory and Design*, ser. Electrical and Computer Engineering. Oxford, U.K.: Oxford Univ. Press, 1998.
- [24] G. Antonini, R. M. Rizzi, and A. Orlandi, "Different strategies for circuit characterization of power delivery networks," in *Proc. Int. Zurich Symp. Electromagnetic Compatibility*, Zurich, Switzerland, Jan. 2009.



Luca De Camillis was born in Teramo, Italy, in 1982. He received the Laurea degree in computer science engineering from the University of L'Aquila in 2007.

From June to December 2008, he was a Research Scientist at the ACE Laboratory, University of Washington, Seattle, focusing on macromodeling techniques and sensitivity analysis applied to high-speed digital boards. He is now with MHT, a software-house working on enterprise resource planning.



Giulio Antonini (M'94–SM'05) received the Laurea degree (*summa cum laude*) in electrical engineering from the Università degli Studi dell'Aquila, in 1994, and the Ph.D. degree in electrical engineering from the University of Rome "La Sapienza," in 1998.

Since 1998, he has been with the UAq EMC Laboratory, Department of Electrical Engineering, University of L'Aquila, where he is currently Associate Professor. His research interests focus on EMC analysis, numerical modeling, and in the field of signal integrity for high-speed digital systems. He has authored or coauthored more than 180 technical papers and two book chapters.

Furthermore, he has given keynote lectures and chaired several special sessions at international conferences. He holds one European patent.

Dr. Antonini was the recipient of the IEEE TRANSACTIONS ON ELECTROMAGNETIC COMPATIBILITY Best Paper Award in 1997, the CST University Publication Award in 2004, the IBM Shared University Research Award in 2004, 2005, and 2006. In 2006, he received a Technical Achievement Award from the IEEE EMC Society "for innovative contributions to computational electromagnetic on the Partial Element Equivalent Circuit (PEEC) technique for EMC applications." He also received the IET-SMT Best Paper Award in 2008. He is vice-chairman of the dell'IEEE EMC Italy Chapter, member of the TC-9 committee, and vice-chairman of the TC-10 Committee of the IEEE EMC Society. He serves as member of the editorial board of *IET Science, Measurements, and Technology*. He serves as reviewer in a number of IEEE journals.



Vikram Jandhyala (S'96–M'00–SM'03) received the B.Tech. degree in electrical engineering from the Indian Institute of Technology (IIT), Delhi, India, in 1993 and the M.S. and Ph.D. degrees from the University of Illinois, Urbana-Champaign, in 1995 and 1998, respectively.

From 1998 to 2000, he was a Research and Development Engineer at Ansoft Corporation, Pittsburgh, PA. Since 2000 he has been a faculty member in the Electrical Engineering Department, as Assistant Professor from 2000 to 2005, and then as tenured Associate Professor. He directs the Applied Computational Engineering (ACE) Lab which has received research funding from DARPA, NSF, SRC, Intel, IBM, NASA, Air Force, Navy, Lawrence Livermore, the SBIR program, and the state of Washington. His research interests include computational electromagnetics, integral equations, fast multilevel algorithms, parallel computation techniques, circuit and system applications of field solvers, signal and power integrity, EMI/EMC, multiphysics and hierarchical simulation methods, RFID systems, statistical and design techniques for field solvers, and graph theory applications of field techniques. He is currently on partial leave from the University of Washington while serving as founder and CEO of Physware, Inc., a venture-funded startup producing electronic design automation tools for microelectronic simulation and design. He has served as a consultant and reviewer for NASA, DoD, NSF, Science Foundation Ireland, Cadence Design Systems, McGraw-Hill, Prentice-Hall, Kluwer, Cambridge University Press, and Calypso Medical. He is a full-elected member of URSI Commission B. He has published approximately 150 papers in journals and refereed conference proceedings.

Dr. Jandhyala is a recipient of a 2008 NASA patent Inventor Award, a 2004 Outstanding Graduate Research Advisor Award from UW EE, a 2001 NSF CAREER award, a Raj Mittra Outstanding Graduate Research Award from UIUC in 1998, and an IEEE Microwave Society Graduate Fellowship in 1997.